Journal Name

ARTICLE

# Two Ruthenium Complexes Capable of Storing Multiple Electrons on a Single Ligand - Photophysical, Photochemical and Electrochemical properties of $[Ru(phen)_2(TAPHAT)]^{2+}$ and $[Ru(phen)_2(TAPHAT)Ru(phen)_2]^{4+}$.

Received 00th January 20xx,
Accepted 00th January 20xx

DOI: 10.1039/x0xx00000x

www.rsc.org/

L. Troian-Gautier,[a]†* L. Marcélis,[b] J. De Winter,[c] P. Gerbaux[c] and C. Moucheron[a]*

The photophysical, photochemical and electrochemical properties of two newly synthesized ruthenium complexes, $[Ru(phen)_2(TAPHAT)]^{2+}$ and $[Ru(phen)_2(TAPHAT)Ru(phen)_2]^{4+}$ is reported. We have developed a novel synthetic methodology that involves the metal-free oxidative coupling of diamino compound to form a desired "pyrazine-type" core. This methodology is employed both on the free diamino ligand as well as on the different ruthenium complexes, illustrating therefore the applicability of this reaction. The TAPHAT ligand, that possesses 7 aromatic rings, 10 nitrogen atoms for 20 carbon atoms gives rise to ruthenium complexes that can undergo up to three consecutive reduction centered on said ligand, a critical parameter for electron storage applications. Temperature dependent study have confirmed the presence of a 4th MLCT state. Excited-state quenching in the presence of guanine or hydroquinone allows to foresee biomedical applications.

## Introduction

Over the past decades, ruthenium(II) polypyridyl complexes have gained much attention due to their peculiar photophysical properties and their applications in various fields such as solar energy conversion, [1] [2] [3] [4] photocatalysis [5] [6] [7] [8] [9] [10] [11] [12] [13] [14] [15] [16] and molecular biology. [17] [18] [19] [20] [21] [22] [23] Ruthenium(II) forms stable octahedral complexes that can be obtained by reaction between a ruthenium precursor and various ligands. Over the years, many efforts have been made to design complexes with fused extended polycyclic ligands. [24] Using complexes bearing these types of ligands allowed many research groups, including ours, to develop complexes with useful applications in the field of biology [25] [26] [27] [28] and photo-catalysis. [4] [29] [30]

Since the seventies, the photophysical scheme of $[Ru(bpy)_3]^{2+}$ has been widely considered as the prototypical one for Ru(II) polypyridyl complexes. [31] [32] [33] [34] Briefly, upon absorption of a photon, a singlet metal-to-ligand charge transfer ($^1$MLCT) excited state is populated. This singlet state is converted within roughly 300 fs to a hot-$^3$MLCT state by efficient intersystem crossing, due to the spin-orbit coupling induced by the heavy atom center. [35] Subsequent vibrational relaxation generates the "Thermally equilibrated excited state", called the THEXI-$^3$MLCT. This excited state can formally be considered as $[Ru(III)(bpy)_2(bpy^{\bullet-})]^{2+*}$. In fact, this emissive $^3$MLCT state corresponds to four low-lying $^3$MLCT states in rapid equilibrium, three of them being separated by 10–90 $cm^{-1}$ while the fourth one is located several hundred $cm^{-1}$ higher in energy. This prototypical photophysical scheme is usually invoked to describe the behavior of the majority of ruthenium(II) complexes. However, the photophysical behavior differs for complexes based on ligands with fused polycyclic rings, such as dipyrido[3,2-a:2',3'-c]phenazine (DPPZ).‡ It was shown that complexes such as $[Ru(bpy/phen)_2(DPPZ)]^{2+}$ behave as light switches, *i.e.* they emit strongly in organic solvent but their luminescence is turned off in aqueous solutions. [25] After numerous discussions and controversies on the possible explanations for this light-switch phenomenon, contributions from Barbara, Papanikolas, Meyer, Lincoln finally resolved the light-switch effect; they proposed a photophysical scheme for $[Ru(bpy)_2(DPPZ)]^{2+}$ in which a non-luminescent state, *i.e.* a "Dark State", is introduced, the energy of which is lower than that of the luminescent $^3$MLCT, *i.e.* the "Bright State", in H-bonding solvents. [36] [37] [38] [39] [40] [41] Further refinements of the model allowed to establish that the "Bright State" corresponds to a charge transfer from the ruthenium center to the 1,10-phenanthroline moiety of the DPPZ ligand, whereas the $^3$MLCT "Dark State" is located on the phenazine moiety of the DPPZ ligand.

Similar phenomena could be observed when the extended ligand PHEHAT (PHEHAT = 1,10-phenanthrolino[5,6-b]1,4,5,8,9,12-hexaazatriphenylene) is used. [27] Interestingly,

[a] Organic Chemistry and Photochemistry, Université libre de Bruxelles (U.L.B.), 50 Av. F.D. Roosevelt, CP 160/08, B-1050 Bruxelles, Belgium.
[b] Engineering of Molecular NanoSystems, Université libre de Bruxelles (U.L.B.), 50 Av. F.D. Roosevelt, CP 165/64, B-1050 Bruxelles, Belgium.
[c] Organic Synthesis and Mass Spectrometry Laboratory, Center of Innovation and Research in Materials and Polymers, Research Institute for Science and Engineering of Materials, University of Mons - UMONS, 23 Place du Parc, B-7000 Mons, Belgium.
† Present Address: Department of Chemistry - Murray Hall, University of North Carolina at Chapel Hill, 123 South Road, Chapel Hill, NC 27599, USA
Electronic Supplementary Information (ESI) available: Structures of mentioned ligands, Photostability, $^1$H-NMR, MS and IR spectra for all new compounds. See DOI: 10.1039/x0xx00000x

the light-switch effect can only be observed when the {Ru(phen)$_2$} moiety is coordinated to the "phen" part of ligand PHEHAT. No light-switch effect is observed when the same moiety is coordinated to the "HAT" part of the same PHEHAT ligand (depicted as HATPHE in this case). [42] Moreover, the study of [Ru(phen)$_2$(PHEHAT)]$^{2+}$ at various temperatures in organic solvent reveals variations of the emission maximum from 720 nm at 220 K to 630 nm at 340 K. The variation between these two wavelengths as a function of temperature was rationalized by the presence of two different luminescent states, of relative low and high energies that are involved in the radiative decay. Nonetheless, the presence of these two luminescent states could not explain all the observed effects. Indeed, when luminescence lifetime is measured as a function of temperature at the two extreme values of wavelength for the maximum in emission (*i.e.* 630 and 720 nm), different behaviors are observed. When the temperature is increased from 290 to 320K, the lifetime measured at 630 nm decreases by 200 ns, whereas a decrease of only 60 ns is observed at 720 nm. Based on these observations, a third state, lower in energy and non-luminescent, was introduced. This lead to a photophysical scheme containing two Bright States in equilibrium with a dark state. Theoretical calculations are in agreement with the experimental data. [43]

In the present work, we report on the first synthesis of a new heptacyclic ligand, TAPHAT for 1,4,5,8-tetraazaphenanthrene[9,10-b]1,4,5,8,9,12-hexaazatriphenylene, (Figure 1) containing ten nitrogen atoms, for only twenty carbon atoms, making it a highly electron-accepting ligand. The use of this ligand allows for the synthesis of the mononuclear [Ru(phen)$_2$TAPHAT]$^{2+}$ complex as well as the symmetrical binuclear [Ru(phen)$_2$(TAPHAT)Ru(phen)$_2$]$^{4+}$ complex. The photophysical properties of these complexes will be compared with those of similar ruthenium(II) polypyridyl complexes.

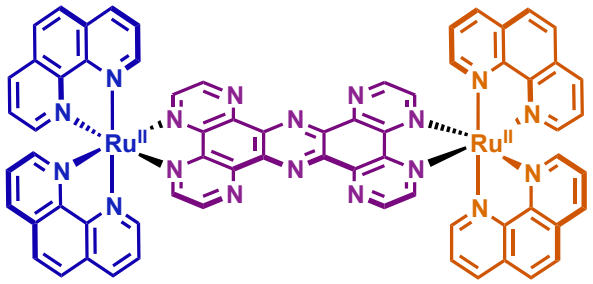


Figure 1. Structure of 1,4,5,8-tetraazaphenanthrene[9,10-b]1,4,5,8,9,12-hexaazatriphenylene (TAPHAT) ligand (purple) as well as [Ru(phen)$_2$(TAPHAT)]$^{2+}$ (Blue-Purple combined) and [Ru(phen)$_2$(TAPHAT)Ru(phen)$_2$]$^{4+}$ (Blue-Purple-Orange combined)

## Results and discussion

### Synthetic procedures

Two synthetic pathways were developed to obtain the desired TAPHAT ligand (Figure 2). The first one proceeds via the condensation reaction between the ligand 1,4,5,8-tetraazaphenanthrene-9,10-diamine (diNH$_2$TAP), already reported in the literature, [27] and the ligand 1,4,5,8-tetraazaphenanthrene-9,10-dione (TAPdione), whose synthesis has never been described. The second strategy involves the self-condensation of diNH$_2$TAP under oxidizing conditions.

The synthesis of diNH$_2$TAP proceeds in four steps, starting from commercially available 1,3,5-trichlorobenzene. Trinitration using potassium nitrate and oleum allows for the isolation of 1,3,5-trichloro-2,4,6-trinitrobenzene. [44] Ammonolysis in toluene yields 1,3,5-triamino-2,4,6-trinitrobenzene [45] that is reduced using Birch-type conditions, *i.e.* metallic sodium in a mixture of methanol and liquid ammonia. [46] This highly reactive species is then reacted with glyoxal, yielding the desired diNH$_2$TAP and 1,4,5,8,9,12-hexaazatriphenylene (HAT) as a side product.

The synthesis of TAPdione proved more difficult as many synthetic pathways did not yield the desired product. Nevertheless, the development of such a ligand is of paramount importance, as it can not only serve for the synthesis of the TAPHAT ligand but can also be used as a key building block for the development of novel ligands and transition metal complexes. The direct oxidation of 1,4,5,8-tetraazaphenanthrene with classical oxidants such as chromium (VI) oxide or potassium permanganate doesn't yield the desired compound, neither does the typical procedure for oxidation of 1,10-phenanthroline into 1,10-phenanthroline-5,6-dione (phendione) using KBr or NaBr in a mixture of nitric acid and sulfuric acid. [47]

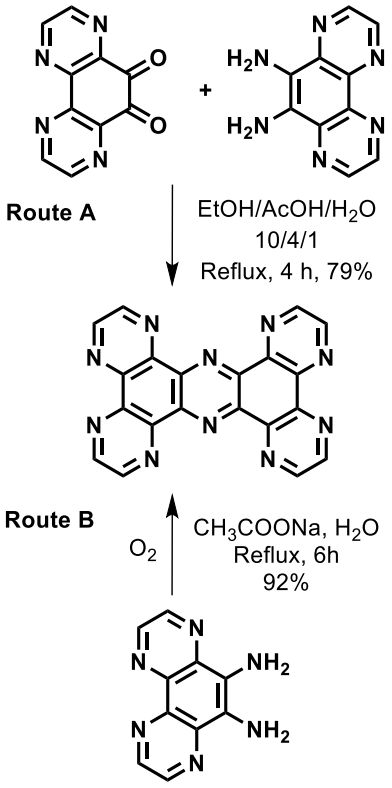


Figure 2. Two strategies investigated in the present work to prepare TAPHAT.

We therefore developed a two-step procedure, starting from 9-methoxy-1,4,5,8-tetraazaphenanthrene (Figure 3), the synthesis of which proceeds in 8 steps starting from 4-fluoro-2-nitro-aniline, as reported in literature. [48] Direct oxidation of 9-

methoxy-1,4,5,8-tetraazaphenanthrene with $MeReO_3$ as reported by Saladino, [49] or with Cerium Ammonium Nitrate, [50] fails to produce the desired 1,4,5,8-tetraazaphenanthrene-9,10-dione. The demethylation of 9-methoxy-1,4,5,8-tetraazaphenanthrene is therefore considered. This reaction is performed with various reagents such as TMSI, [51] $BBr_3$, [52] [53] EtSH, [54] sodium in hexamethylphosphoramide [55] and hydrogen iodide. Among all the reagents that were tested, only demethylation with hydrogen iodide allows for the isolation of 9-hydroxy-1,4,5,8-tetraazaphenanthrene with an 85% yield. The last step is the oxidation of phenol to the corresponding *ortho*-quinone using a hypervalent iodine compound. [56] For this oxidation, (bisacetoxy)iodobenzene is selected as we have previously shown that this oxidant does not react with the quinoxaline core, but only with the phenolic group. [56] This reaction allows obtaining the desired 1,4,5,8-tetraazaphenanthrene-9,10-dione in an 83% yield. (Figure 3).

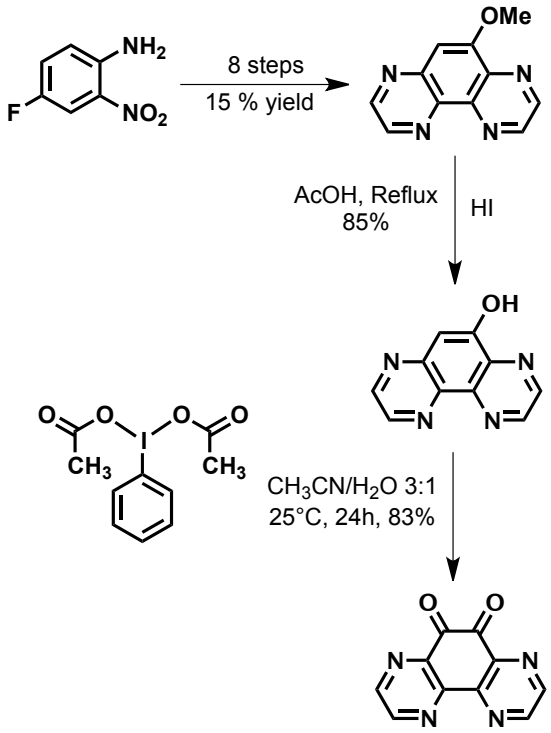


Figure 3. Synthesis of 1,4,5,8-tetraazaphenanthrene-9,10-dione

With **diNH$_2$TAP** and **TAPdione** in hand, the two synthetic routes to obtain the TAPHAT ligand are explored.

The first strategy consists in the condensation of the dione and the diamine in a mixture of ethanol/water/acetic acid 10/4/1. The reaction allows to recover the desired product with a 79% yield. The formation of a supplementary aromatic ring combined with the precipitation of the desired compound over time are key factors for the obtained yields and allows easy recovery of the desired product. The second strategy is inspired by the reaction described in 2000 by Gajiwala and Zand. [57] For this reaction, **diNH$_2$TAP** is dissolved in hot water in the presence of sodium acetate. Oxygen is continuously bubbled through the solution for 6 h. The color of the mixture is rapidly observed to fade while a precipitate is formed. This green and efficient method allows to isolate the desired compound with a yield of 92%. Both reaction pathways yield TAPHAT as a grey solid, insoluble in all classical solvents, and therefore preventing characterization through classical techniques such as $^{1}H/^{13}C$ NMR.

Due to its poor solubility, and its four different chelation sites, the design of a synthetic path that would only yield $[Ru(phen)_2(TAPHAT)]^{2+}$ or $[Ru(phen)_2(TAPHAT)Ru(phen)_2]^{4+}$ starting from the free ligand TAPHAT is not straightforward. By reacting TAPHAT with the precursor $[Ru(phen)_2Cl_2]$, a mixture of mono- and dinuclear complexes is obtained, as indicated by mass spectrometry measurements (**Figure S2**). Separation of these two complexes by conventional purification methods is tedious, encouraging us to develop an alternative synthetic procedure based on the precursor complex $[Ru(phen)_2(diNH_2TAP)]^{2+}$, the synthesis of which being already reported in literature. [42] Mononuclear $[Ru(phen)_2(TAPHAT)]^{2+}$ **1** is obtained by two different procedures. The first one consists in reacting $[Ru(phen)_2(diNH_2TAP)]^{2+}$ with **TAPdione** in an ethanol/water 7/3 mixture. The desired compound is isolated with a moderate yield of 42% after column chromatography on alumina. The second strategy takes advantage of the method developed by Gajiwala and Zand. Reacting $[Ru(phen)_2(diNH_2$-$TAP)]^{2+}$ with an excess of **diNH$_2$TAP** in water while bubbling oxygen for 6 h produces the desired complex with a yield of 93 %, and the ligand TAPHAT as the side product.

The binuclear $[Ru(phen)_2(TAPHAT)Ru(phen)_2]^{4+}$ **2** is also synthesized by bubbling oxygen in water containing sodium acetate and the precursor $[Ru(phen)_2(diNH_2TAP)]^{2+}$ complex. After bubbling oxygen for 8 h, ammonium hexafluorophosphate is added to precipitate the complex that is washed several times with water to obtain the symmetrical dinuclear complex **2** with a 95 % yield.

**Electrochemistry**

For classical ruthenium(II) polypyridyl complexes, it is generally accepted that the reduction processes are ligand centered whereas the oxidation processes are metal centered. The redox potential can be tuned by varying the polypyridyl ligands that are chelated to the ruthenium center. The introduction of nitrogen atoms in the polypyridyl backbone will lead to more π-accepting ligands and, as a consequence, the resulting complexes will be easier to reduce and harder to oxidize. The TAPHAT ligand, with its ten nitrogen atoms for twenty carbon atoms should be a highly π-accepting ligand, and therefore make the complexes easy to reduce and difficult to oxidize. Electrochemical data obtained by square-wave voltammetry (Figure 4) for complexes **1** and **2** are reported in Table 1 as well as values from representative complexes.

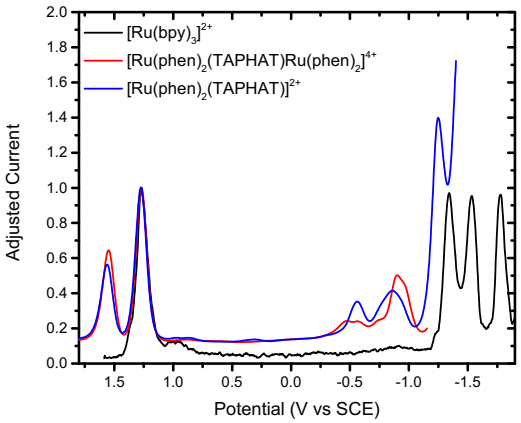


Figure 4. Square-wave voltammograms for $[Ru(phen)_2(TAPHAT)]^{2+}.2PF_6^-$ (**1**), $[Ru(phen)_2(TAPHAT)Ru(phen)_2]^{4+}.4PF_6^-$ (**2**) and $[Ru(bpy)_3]^{2+}.2PF_6^-$ measured in 0.1M $TBAClO_4$ acetonitrile solution. $[Ru(bpy)_3]^{2+}.2PF_6^-$ was used as an internal reference.

Table 1. Redox potentials measured in acetonitrile solutions for complexes **1** and **2** (0.1 M $TBAClO_4$) and reference Ru(II) polypyridyl complexes (0.1 M $TBAPF_6$).

| Complex | Oxidation V vs SCE | Reduction V vs SCE |
|---|---|---|
| $[Ru(phen)_3]^{2+}$ [58] | +1.29 | -1.35; -1.52 |
| $[Ru(phen)_2(HAT)]^{2+}$ [59] | +1.53 | -0.86; -1.42; -1.69 |
| $[Ru(phen)_2(PHEHAT)]^{2+}$ [42] | +1.35 | -1.00; -1.25 |
| $[Ru(phen)_2(HATPHE)]^{2+}$ [42] | +1.56 | -0.83; -1.01 |
| $[Ru(phen)_2(TPPHZ)]^{2+}$ [60] | +1.34 | -1.00; -1.38; -1.69 |
| $[(phen)_2Ru(HAT)Ru(phen)_2]^{4+}$ [59] | +1.52 +1.78 | -0.49; -1.07 |
| $[Ru(phen)_2(PHEHAT)Ru(phen)_2]^{4+}$ [61] | +1.34 +1.55 | -0.68; -1.06 |
| $[(phen)_2Ru(TPPHZ)Ru(phen)_2]^{4+}$ [60] | +1.34 (2) | -0.78; -1.36(2); -1.52 |
| **1** | +1.56 | -0.56; -0.86[(a)]; -1.26 |
| **2** | +1.55 (2) | -0.52; -0.90[(a)] |

(a) Broad signal that corresponds to two close reduction waves. In oxidation, (2) depicts two-electrons waves.

Mononuclear complex **1** exhibits an oxidation at +1.56 V *vs* SCE, which agrees with expected values. When the ruthenium center is chelated to two 1,10-phenanthroline ancillary ligands and one π-accepting ligand such as HAT (1,4,5,8,9,12-hexaazatriphenylene) or HATPHE (*i.e.* $[Ru(phen)_2(HAT)]^{2+}$ and $[Ru(phen)_2(HATPHE)]^{2+}$), the oxidation wave is indeed centered around +1.5 V *vs* SCE. In the case of the binuclear complex $[Ru(phen)_2(TAPHAT)Ru(phen)_2]^{4+}$ **2**, an oxidation wave is observed at +1.55 V *vs* SCE. The observation of one bi-electronic oxidation wave at a unique potential indicates that the two ruthenium(II) centers are oxidized simultaneously, which means that they behave independently. A similar behavior can be observed for the binuclear complex based on the TPPHZ (tetrapyrido[3,2-a: 2',3'-c: 3'',2-h: 2''',3'''-j]phenazine) ligand, where the Ru(II) centers are independent.

Regarding the reduction potentials, we obtain values of -0.56 V, -0.86 V (which corresponds to two close reduction waves), and -1.26 V *vs* SCE for mononuclear $[Ru(phen)_2(TAPHAT)]^{2+}$ **1**. Reduction waves associated with the reduction of 1,10-phenanthroline ancillary ligands only appear at values more negative than -1.35 V *vs* SCE. Indeed, the complex $[Ru(phen)_3]^{2+}$ exhibits a first reduction wave at -1.35V *vs* SCE, whereas the complex $[Ru(phen)_2(HAT)]^{2+}$ exhibits its first reduction wave centered on the 1,10-phenanthroline ligand at -1.42 V *vs* SCE. This implies that the two first reduction waves observed can be unambiguously attributed to the successive addition of three electrons on the TAPHAT ligand. The value of -0.56V *vs* SCE is, to the best of our knowledge, the less negative value obtained for a mononuclear complex based on heptacyclic ligands of this type and having two ancillary phen ligands. [62] The value at -1.26V *vs* SCE could correspond to a fourth reduction of the TAPHAT ligand, but at these potentials, adsorption and irreversible processes are observed which prevent a complete assessment of this hypothesis. Thus, at this stage, the fourth reduction wave observed for complex **1** could not be attributed with certainty to either the TAPHAT ligand or the ancillary 1,10-phenanthroline ligand. Concerning the binuclear complex $[Ru(phen)_2(TAPHAT)Ru(phen)_2]^{4+}$ **2**, the reduction waves are observed at -0.52V, -0.90V (which corresponds to two close reduction waves). Once again, the three first waves can be confidently attributed to successive reductions of the TAPHAT ligand. It should also be noted that when scanning at potentials more negative than the third reduction, irreversible processes occurred that were either due to adsorption of the complexes to the electrode or to degradation of complexes **1** and **2**. The fact that these reduction processes as well as the oxidation occur at similar potentials for complexes **1** and **2** is a clear evidence of the lack of coupling between the two ruthenium centers that behave independently. [24] [62]

Multiple electron storage has already been reported in the literature for ruthenium complexes based on fused polycyclic ligands such as disubstituted DPPZ, [63] dph, [62] tatpp [64] [65] and tatpq, [66] [67] but never to such extent. DPPZ based complexes can undergo two reduction processes centered on the DPPZ ligand, [63] whereas tatpp an tatpq can either undergo a two electron reduction process or multiple electronic processes when the tatpp ligand is bridged. [65] For complexes **1** and **2**, this unprecedented three electron reduction is a direct consequence of the high π-accepting character of the TAPHAT ligand. Control experiments were performed by diluting the concentration of **1** and **2** to confirm that these reductive processes are a direct consequence of the TAPHAT ligand and not due to π-stacking leading to erroneous electrochemical data.

**Absorption**

The UV/visible absorption spectra of complexes **1** and **2** measured in acetonitrile are presented in Figure 5.

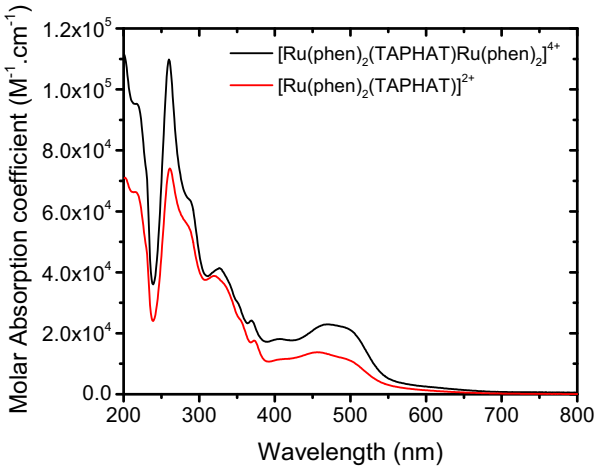


Figure 5. Absorption spectra of $[Ru(phen)_2(TAPHAT)]^{2+}.2PF_6^-$ (red) and $[Ru(phen)_2(TAPHAT)Ru(phen)_2]^{4+}.4PF_6^-$ (black) complexes in acetonitrile.

Both ruthenium(II) complexes **1** and **2** present absorption spectra typical of ruthenium complexes. The absorption spectrum of the dinuclear species is similar to that of the mononuclear one, only with higher absorption coefficient, as is expected for a dinuclear complex. The absorption feature between 400 nm and 600 nm is attributed to metal to ligand charge transfer (MLCT) transitions, whereas features below 400 nm are generally attributed to ligand centered (LC) transitions. For both complexes, an absorption feature at 380 nm is observed; this transition is characteristic of a LC transition for complexes bearing a ligand with extended fused polycyclic units, as observed for complexes bearing DPPZ, [25] TPPHZ [68 69] or PHEHAT [61] ligands. Absorption maxima and molar absorption coefficients for the MLCT transition for complexes **1** and **2** are presented in Table 2, along with those of a series of Ru(II) complexes bearing extended planar ligands for sake of comparison.

It should be noted that $[Ru(phen)_2(PHEHAT)]^{2+}$ has an absorption coefficient of 22700 $M^{-1}.cm^{-1}$ at 438 nm while the complex $[Ru(phen)_2(HATPHE)]^{2+}$ has an absorption coefficient of 14700 $M^{-1}.cm^{-1}$ at 428 nm. Thus, when the PHEHAT ligand is used, the absorption coefficient varies drastically depending on which moiety, "phen" or "HAT", of the ligand is coordinated to the ruthenium(II) ion. Based on the comparison with other complexes, it is observed that $[Ru(phen)_2(TAPHAT)]^{2+}$ has an absorption coefficient of 13700 $M^{-1}.cm^{-1}$ at 460 nm, which is a value close to that of $[Ru(phen)_2(HATPHE)]^{2+}$ or $[Ru(phen)_2(HAT)]^{2+}$, suggesting a similar oscillator strength for this transition involving a π-deficient moiety. The value of the absorption coefficient thus supports the assignment of the excited state to a $^3$MLCT localized on the HAT moiety of the bridging TAPHAT ligand.

Regarding the binuclear complex **2**, the absorption coefficient is 22400 $M^{-1}.cm^{-1}$ at 460 nm. This value is smaller than the values for other binuclear species based on the PHEHAT ligand gathered in Table 2. When considering the complexes $[Ru(phen)_2(HAT)]^{2+}$ and $[Ru(phen)_2(HAT)Ru(phen)_2]^{2+}$, the absorption coefficient increases from 14000 $M^{-1}.cm^{-1}$ for the mononuclear species to 19700 $M^{-1}.cm^{-1}$ for the dinuclear species. This enhancement of the absorption coefficient is moderate compared to the one observed for complexes **1** and **2**. Along with the absence of a bathochromic shift for the binuclear complex, it can be concluded that, in agreement with the behavior observed in electrochemistry, the two Ru(II) centers behave independently.

**Steady-State Photoluminescence**

Steady state photoluminescence studies were performed in various solvents in order to highlight the influence of medium polarity on the excited states of these two complexes. The emission spectra, recorded in water, methanol, acetonitrile, acetone and dichloromethane at 298K under air are presented in Figure 6 for complexes **1** (top) and **2** (bottom). The emission maxima are gathered in Table 3, as well as those of complexes reported in the literature for comparison.

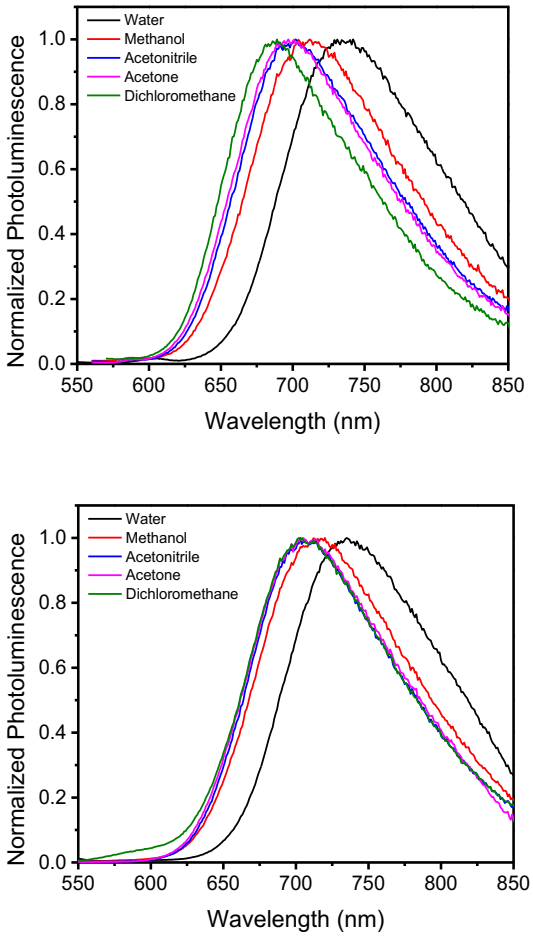


Figure 6. Steady state photoluminescence spectra of complexes **1** (top) and **2** (bottom). These spectra were recorded at room temperature in water (black), methanol (red), acetonitrile (blue), acetone (pink) and dichloromethane (green). Absorption of the different complexes was kept below 0.1 to avoid inner filter effects. The steady-state photoluminescence spectra were corrected for the instrument response. Chloride counter-ions were used for measurements in water and methanol whereas $PF_6^-$ counter-ions were used for measurements in acetonitrile, acetone and dichloromethane.

Table 2. Absorption characteristics of complexes $Ru(phen)_2(TAPHAT)]^{2+}$ and $[Ru(phen)_2(TAPHAT)\ Ru(phen)_2]^{4+}$ in acetonitrile, compared to other complexes based on HAT and PHEHAT ligands.

| Complex | $\lambda_{max}$ absorption (nm) | Absorption Coefficient ($M^{-1}.cm^{-1}$) | Chromophore (MLCT)[a] |
|---|---|---|---|
| **1** | 220, 260, 290, 330, 370, 410, 460, 500 | 13700 | Ru-TAPHAT |
| **2** | 220, 260, 290, 330, 390, 410, 460, 500 | 22400 | Ru-TAPHAT |
| $[Ru(phen)_3]^{2+}$ | 262, 418, 447 | 18400 | Ru-phen |
| $[Ru(phen)_2(HAT)]^{2+}$ [61] | 262, 420, 480$^{sh}$ | 14000 | Ru-HAT |
| $[Ru(phen)_2(HAT)Ru(phen)^2]^{4+}$ [59] | 220$^{sh}$, 262, 358$^{sh}$, 406, 490, 564 | 19700 | Ru-HAT-Ru |
| $[Ru(phen)_2(PHEHAT)]^{2+}$ [27] | 264, 278$^{sh}$, 312$^{sh}$, 354, 370, 438 | 22700 | Ru-PHEHAT |
| $[Ru(phen)_2(HATPHE)]^{2+}$ [42] | 260, 288$^{sh}$, 316, 364, 382, 428, 478$^{sh}$ | 14700 | Ru-HATPHE |
| $[Ru(phen)_2(PHEHAT)Ru(phen)^2]^{4+}$ [61] | 261, 288$^{sh}$, 309$^{sh}$, 330$^{sh}$, 368, 420$^{sh}$, 444, 475$^{sh}$ | 28100 | Ru-HATPHE |

[a] The molar absorption coefficient listed correspond to the MLCT band (underlined).

Table 3. Photoluminescence maxima (± 1nm) measured under air in different solvents at 298K.

| | Water $\varepsilon_r = 79$ $\lambda_{max}$ (nm) | Methanol $\varepsilon_r = 33$ $\lambda_{max}$ (nm) | Acetonitrile $\varepsilon_r = 38$ $\lambda_{max}$ (nm) | Acetone $\varepsilon_r = 21$ $\lambda_{max}$ (nm) | DCM $\varepsilon_r = 9$ $\lambda_{max}$ (nm) |
|---|---|---|---|---|---|
| **1** | 742 | 712 | 702 | 697 | 689 |
| **2** | 735 | 720 | 703 | 705 | 702 |
| $[Ru(phen)_3]^{2+}$ [42 70] | 604 | 594 | 604 | | |
| $[Ru(phen)_2(HAT)]^{2+}$ [42] | 732 | | 696 | | |
| $[Ru(phen)_2(PHEHAT)]^{2+}$ [42] | -[a] | -[a] | 662 | 639 | 606 |
| $[Ru(phen)_2(HATPHE)]^{2+}$ | 730 | 723 | 692 | 693 | 680 |

[a] not luminescent.

In contrast to the well-known $[Ru(bpy)_2(dppz)]^{2+}$ and $[Ru(phen)_2(PHEHAT)]^{2+}$, which behave as light-switches, complexes based on the TAPHAT ligand are luminescent in both hydroxylated and organic solvents. As for other polypyridyl complexes, a distinct solvatochromism is observed; *i.e.* a red-shift of 40 nm and 32 nm for complexes **1** and **2** respectively in the emission maxima when switching from acetonitrile to water. This solvatochromism confirms the charge transfer character of the excited state of these complexes. Furthermore, in agreement with the electrochemical data, this charge transfer state is assigned to a $^3$MLCT excited state localized on the TAPHAT moiety. This conclusion can be drawn by comparing the emission maxima with those for complexes such as $[Ru(phen)_2(HAT)]^{2+}$, $[Ru(phen)_3]^{2+}$ and $[Ru(phen)_2(PHEHAT)]^{2+}$. Indeed, $[Ru(phen)_2(HAT)]^{2+}$ emits at 732 nm in water and 696 nm in acetonitrile when decaying from its $^3MLCT_{Ru\text{-}HAT}$ excited state, while $[Ru(phen)_3]^{2+}$ emits at 604 nm in water as well as in acetonitrile. Thus, a Ru-HAT transition is much less energetic than a Ru-phen transition, and is more sensitive to the solvent. The behavior of complex **1** is similar to that of $[Ru(phen)_2(HATPHE)]^{2+}$, whose emission values have been recorded here in different solvents, in contrast to $[Ru(phen)_2(PHEHAT)]^{2+}$, which is non-emissive in both water and methanol. Nonetheless, in organic solvents a bathochromic shift is observed when changing from $[Ru(phen)_2(PHEHAT)]^{2+}$ to $[Ru(phen)_2(TAPHAT)]^{2+}$. This is in agreement with a $^3$MLCT state localized on a close "HAT" moiety of the TAPHAT ligand or on the whole ligand. Similar observation can be made for complex **2**.

The data also suggest that mononuclear complex **1** is more sensitive to polarity than binuclear complex **2**. Indeed, a blue shift of 53 nm for the mononuclear complex **1** is observed when going from water to dichloromethane while the blue shift is only 33 nm for the binuclear complex **2**. Furthermore, the differences in the maximum emission wavelengths observed in acetonitrile, acetone and dichloromethane are much more pronounced for the mononuclear complex **1** than for the binuclear complex **2**. It is important to notice that for the binuclear complex, solvent molecules only have access to the "terpyrazine-like" moiety of ligand TAPHAT, whereas in the mononuclear complex, the bidentate coordination site is still accessible. Also the dipole moment of the excited-state of complex **1** and **2** is expected to be of different intensity, and thus, the potential sites for solvent interaction might not be the only contributing factor for the observed solvatochromism. To gain further insight into the behavior of these excited states, we investigated how the luminescence lifetimes change according to solvent polarity.

**Luminescence lifetime and Quantum Yield**

The emission lifetimes and luminescence quantum yields (Table 4) for $[Ru(phen)_2(TAPHAT)]^{2+}$ **1** and

 

$[Ru(phen)_2(TAPHAT)Ru(phen)_2]^{4+}$ **2** were determined at 298K in various solvents. Luminescence lifetimes are measured under air and under argon. As expected, the influence of oxygen is more pronounced in organic solvents, as it is more soluble in these than in water.

The luminescence lifetimes (and the quantum yield of luminescence) of complexes **1** and **2** decrease as solvent polarity increases, in agreement with a greater stabilization of charge transfer states in more polar solvents and the energy gap law.

It should be noted that a shorter lifetime in acetonitrile compared to water is observed for complexes such as $[Ru(TAP)_3]^{2+}$ and $[Ru(HAT)_3]^{2+}$. [71] This observation is explained by a thermal activation from the luminescent $^3$MLCT towards a non-luminescent $^3$MC state, constituting an important deactivation pathway that can lead to photo-release of ligand. For those complexes, a stabilization of the $^3$MLCT in polar solvent increases the energy gap for the $^3$MLCT-$^3$MC transition, leading to an increase of the $^3$MLCT lifetime. For complexes **1** and **2**, the presence of 1,10-phenanthroline ancillary ligands, considered as σ-donor ligands, increases the $^3$MLCT-$^3$MC energy gap, which makes deactivation via the $^3$MC state harder for these complexes. This correlates with the observed stability of both complexes under irradiation (**Figure S10**).

It is also noticed that the lifetimes are even shorter in solvents capable of H-bonding, such as methanol and water, than in non H-bonding solvents. In order to assess the possible influence of the number of non-chelated nitrogen atoms capable of H-bonding on the stabilization of the excited states of complexes **1** and **2**, their emission lifetimes were measured in $D_2O$. It is well-known for $[Ru(bpy)_3]^{2+}$ that its excited state lifetime is enhanced in deuterated water. This is, in this case, solely due to the difference between OH and OD oscillators; OD are less efficient energy acceptor oscillators than OH, yielding less efficient non-radiative decay for the excited complex. [72]

Since **1** and **2** are capable of H/D-bonding with solvent, a change in their excited state lifetime could also be observed when switching to deuterated water. Changes in lifetime will, in that case, mainly reflect the change in H/D-bonds between $H_2O/D_2O$ and the non-chelated nitrogen atoms. The excited-state lifetime is increased for both complexes **1** and **2** in $D_2O$, but the effect is more pronounced for the mononuclear complex **1**. An excited-state lifetime of 219 ns in $D_2O$ vs 118 in $H_2O$ was measured while in contrast, the exited-state lifetime of **2** only evolves from 124 ns in $H_2O$ to 136 ns in $D_2O$. These $(H/D)_2O$ measurements suggest that the number of non-chelated nitrogen atoms plays an important role in the stabilization of the excited state.

From the lifetime measurements and the luminescence quantum yields, it is possible to calculate the radiative and non-radiative deactivation constants. These values are summarized for complexes **1** and **2** in Table 5. Radiative and non-radiative deactivation constants for complex $[Ru(phen)_2(HATPHE)]^{2+}$ are also measured and are reported in Table 5 for discussion purposes. This complex is chosen because its lowest excited state is localized on the extended ligand, which is also the case for the complexes presented in this paper. Furthermore, this complex exhibits absorption features that are similar to those for complexes based on TAPHAT ligand. $[Ru(phen)_2(HATPHE)]^{2+}$ displays steady state photoluminescence that is appreciable in each solvent used in the present work.

The radiative and non-radiative deactivation constants follow the expected trend; the high non-radiative deactivation constants result in a decrease of the excited state lifetimes in polar solvents ($\tau = 1/(k_r + k_{nr})$), because this deactivation constant increases in an inversely proportional manner with the energy gap law coupled to the fact that these $^3$MLCT states are more stabilized in polar solvents.

Table 4. Photoluminescence lifetimes and quantum yields for complexes **1** and **2** in various solvents. Chloride counter-ions were used for measurements in water and methanol whereas $PF_6^-$ counter-ions were used for measurements in acetonitrile, acetone and dichloromethane.

| | $\varepsilon_r$ | $O_2$ sol. (x $10^{-3}$M) | $[Ru(phen)_2(TAPHAT)]^{2+}$, **1** | | | | $[Ru(phen)_2(TAPHAT)Ru(phen)_2]^{4+}$, **2** | | | |
|---|---|---|---|---|---|---|---|---|---|---|
| | | | τ (ns) | | Φ | | τ (ns) | | Φ | |
| | | | Air | Argon | Air | Argon | Air | Argon | Air | Argon |
| Water | 79 | 0.278 | 113 | 118 | 0.007 | 0.008 | 122 | 124 | 0.008 | 0.009 |
| Methanol | 33 | 1.95 | 260 | 360 | 0.010 | 0.011 | 252 | 353 | 0.015 | 0.020 |
| Acetonitrile | 38 | 2.42 | 356 | 600 | 0.019 | 0.028 | 315 | 532 | 0.020 | 0.027 |
| Acetone | 21 | 2.37 | 370 | 650 | 0.019 | 0.022 | 325 | 548 | 0.024 | 0.034 |
| Dichloromethane | 9 | 2.2§ | 690 | 710 | 0.027 | 0.030 | 617 | 898 | 0.027 | 0.028 |

Measurements were performed at room temperature in water, methanol, acetonitrile, acetone and dichloromethane, under air and under argon. Absorption of the different complexes was kept below 0.1 to avoid inner filter effects. Uncertainties in the excited-state lifetimes are 5%. Dielectric constant and concentration of dissolved oxygen are listed for each solvent. [73]

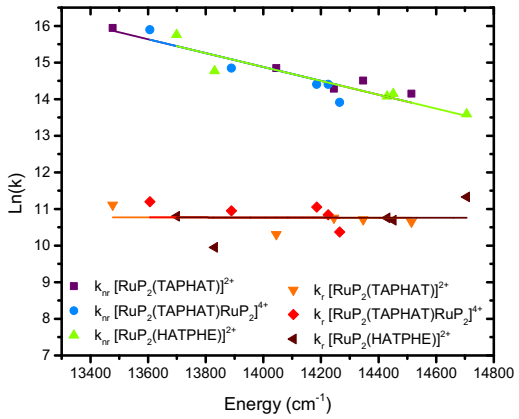


Figure 7. Energy Gap Law plot of the radiative and non-radiative deactivation constants measured in different solvents for $[Ru(phen)_2(TAPHAT)]^{2+}$, $[Ru(phen)_2(TAPHAT)Ru(phen)_2]^{4+}$ and $[Ru(phen)_2(HATPHE)]^{2+}$

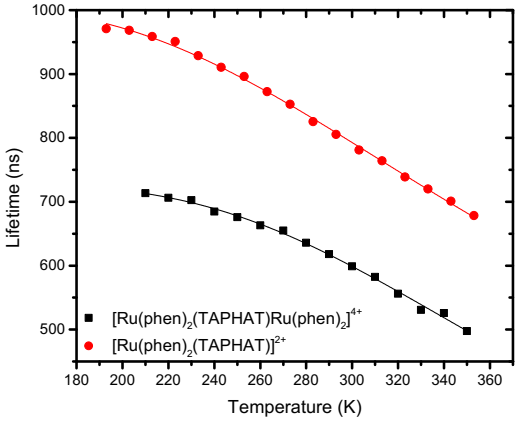


Figure 8. Luminescence lifetime of $[Ru(phen)_2(TAPHAT)]^{2+}.2PF_6^-$ (red) and $[Ru(phen)_2(TAPHAT)Ru(phen)_2]^{4+}.4PF_6^-$ (black) in butyronitrile measured under argon between 350 and 190 K.

A linear correlation is obtained when plotting the natural logarithm of the non-radiative or radiative rate constant as a function of the photoluminescence maximum in energy. These linear fittings (Figure 7) confirm that the energy gap Law is respected and similar for the complexes studied here.

**Luminescence lifetime as a function of temperature**

In $[Ru(bpy)_3]^{2+}$, the absorption of a photon leads to the population of a $^1$MLCT that decays rapidly (300 ps) to a "Thermally equilibrated excited state" THEXI-$^3$MLCT state by intersystem crossing (ISC). [35] Studies by Crosby *et al.* revealed that this $^3$MLCT state is in fact composed of three low-lying MLCT states in rapid equilibrium that are separated by 10–90 $cm^{-1}$. [31] These states can only be distinguished at 77 K. Von Zelewsky and Meyer have later identified that a fourth MLCT with greater singlet character is also present at several hundred $cm^{-1}$ to higher energy. [74] [75] [33] [76] In the absence of excited-state quenching, the THEXI-$^3$MLCT state can deactivate through radiative or non-radiative decay, or through thermal activation leading to a metal-centered state ($^3$MC) also termed Ligand-Field state (LF) or d-d state. Population of these $^3$MC states can lead to ligand loss or ligand substitution. This photophysical scheme is often accepted as the model for all homoleptic complexes and for several heteroleptic complexes although several examples contradict this photophysical scheme. [77] [78] To understand the photophysical scheme that is at stake for **1** and **2**, we performed temperature dependent time-resolved photoluminescence measurements in butyronitrile (Figure 8).

The data presented in Figure 8 are modelled using a modified Arrhenius analysis as reported by Van Houten and Watts (eq.1). [72]

$$\tau^{-1} = k_r + k_{nr} + A \exp\left(-\frac{E_a}{RT}\right) \quad \text{(eq.1)}$$

Relaxation of the THEXI-$^3$MLCT state to an upper $^3$MC state is expected to occur with energy activation that ranges from 2000 to 5000 $cm^{-1}$ depending on the nature of the ligands as well as the polarity of the solvent that influences the THEXI-$^3$MLCT state energetics. [74] [75] [33] [76] These activation energies are often accompanied by very large preexponential factors ($10^{10}$-$10^{15}$ $s^{-1}$). [76] [79] [80] When the THEXI-$^3$MLCT state relaxes to a 4$^{th}$ MLCT excited state, these energies are usually centered between 400 and 1000 $cm^{-1}$ with smaller preexponential factors ($10^6$-$10^9$ $s^{-1}$). [81] [75] The values obtained from the temperature dependent time-resolved photoluminescence measurements are summarized in Table 6, with A being the preexponential factor, $k_i$ being the sum of $k_r$ and $k_{nr}$, and $E_a$ corresponding to the activation energy. Based on the weak activation energy and the relatively small preexponential factors, we propose that this thermally activated pathway involves a 4$^{th}$ MLCT state. This is also confirmed by the photostability measurements which show that both complexes **1** and **2** are photostable (**Figure S10**). Thus, we can conclude that this thermally activated pathway corresponds to a deactivation through a 4$^{th}$ MLCT rather than a $^3$MC excited state.

The photoluminescence of complexes **1** and **2** was recorded in frozen butyronitrile glass at 77K (figure 9). Franck-Condon lineshape analysis allowed to extrapolate parameters such as the vibrational mode for relaxation, the band maximum of the first medium frequency progression ($E_{0\text{-}0}$) as well as the Huang-Rhys factor ($S_M$). [82] [83] [84] The Huang-Rhys factor is often associated with the reorganization energy and the frequency of the quantum mode. A vibrational mode of 1240 $cm^{-1}$ and 1297 $cm^{-1}$ for complexes **1** and **2** respectively could be determined, indicating therefore a common relaxation pathways for these two complexes. This value is very similar to that of $[Ru(bpy)_3]^{2+}$ suggesting therefore relaxation

through a common Ruthenium-polypyridyl vibrational mode. [85] [86] [87] Huang-Rhys factors of 0.65 and 0.82 for **1** and **2** respectively indicated that the final and initial states of these two complexes coincide along the normal coordinate. $E_{0\text{-}0}$ can usually be determined using the $\lambda_{max}$ of emission, which corresponds to an underestimated value, or by using the x-intercept of a linear extrapolation of the blue edge of the corrected emission spectra. This technique usually yields $E_{0\text{-}0}$ that are closer to the true value. Franck-Condon Lineshape analysis provides $E_{0\text{-}0}$ that are more accurate than the two previously mentioned techniques but requires steady-state photoluminescence measurements in frozen glass. $E_{0\text{-}0}$ values of 15330 $cm^{-1}$ (652 nm) and 15410 $cm^{-1}$ (649 nm) for complexes **1** and **2** were determined using such analysis. These values correspond to the energy difference between the ground and excited state, both taken at their zero vibrational levels.

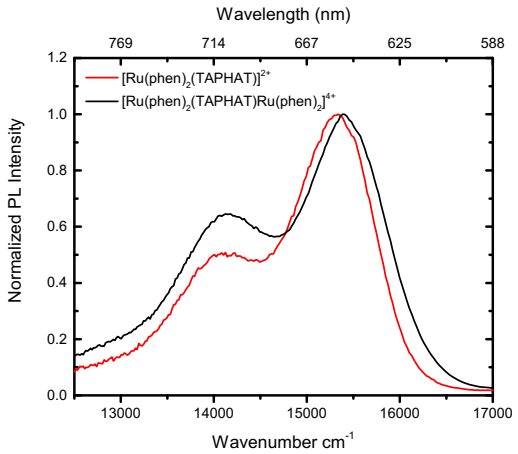


Figure 9. Steady-State photoluminescence of $[Ru(phen)_2(TAPHAT)]^{2+}.2PF_6^-$ (red) and $[Ru(phen)_2(TAPHAT)Ru(phen)_2]^{4+}.4PF_6^-$ (black) recorded in frozen butyronitrile glass at 77K.

### Excited-State Quenching

Based on the relatively positive reduction potential of the two photostable complexes discussed in this work, we investigated their ability to react in their excited state with two reductants, hydroquinone ($H_2Q$, $E_{ox}$ = +0.46 V *vs* SCE [88]) and guanosine-5'-monophosphate (GMP, $E_{ox}$ = +1.07 V *vs* SCE [89]) [90], allowing therefore a 600 mV driving force range to be investigated. We also determined the quenching constant for complexes such as $[Ru(phen)_2(HAT)]^{2+}$, $[Ru(phen)_2(TAP)]^{2+}$ and $[Ru(phen)_3]^{2+}$ with hydroquinone in order to discuss the influence of the π-accepting ligand TAPHAT. These results are presented in Figure 10 and the corresponding quenching constants are summarized in Table 7.

The quenching rate constants for the different systems developed in this study followed the same trend as the excited-state reduction potentials. As expected, for $[Ru(phen)_3]^{2+}$ there is no appreciable photo-induced electron transfer with hydroquinone. The addition of just one π-accepting ligand allows the photo-induced electron transfer to take place from the reductant to the excited state of the complex. Importantly, complexes based on the TAPHAT ligand exhibit relatively high quenching rate constants compared to similar complexes bearing 1,10-phenanthroline ancillary ligands. This is still more noticeable with GMP as the reductant, where the quenching rate constant is 30 times higher with $[Ru(phen)_2(TAPHAT)]^{2+}$ ($k_q$ = 6.24 $10^8$ $M^{-1}.s^{-1}$) than it is with $[Ru(phen)_2(HAT)]^{2+}$ ($k_q$ = 0.24 $10^8$ $M^{-1}.s^{-1}$).

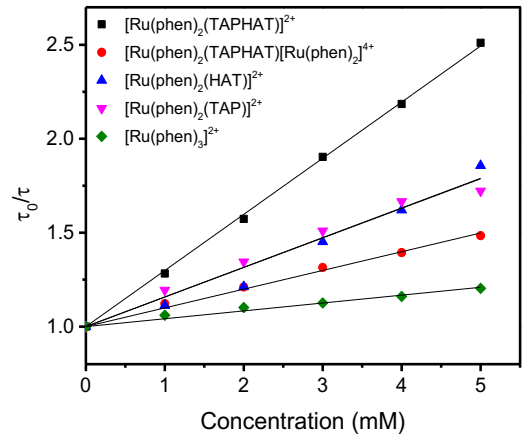


Figure 10. Stern-Volmer plot representing the quenching of the excited state of various ruthenium$^{II}$ complexes by hydroquinone. Measurements were carried out under air at pH 5 in the presence of 150 mM sodium chloride and 10 mM phosphate buffer.

Table 5. Radiative and non-radiative rate constants for complex $[Ru(phen)_2(TAPHAT)]^{2+}$ **1**, $[Ru(phen)_2(TAPHAT)Ru(phen)_2]^{4+}$ **2** and $[Ru(phen)_2(HATPHE)]^{2+}$ under argon. Chloride counter-ions were used for measurements in water and methanol whereas $PF_6^-$ counter-ions were used for measurements in acetonitrile, acetone and dichloromethane.

| | $[Ru(phen)_2(TAPHAT)]^{2+}$ **1** | | $[Ru(phen)_2(TAPHAT)\ Ru(phen)_2]^{4+}$**2** | | $[Ru(phen)_2(HATPHE)]^{2+}$ | |
|---|---|---|---|---|---|---|
| | $k_r$ (x $10^4$ $s^{-1}$) | $k_{nr}$ (x $10^6$ $s^{-1}$) | $k_r$ (x $10^4$ $s^{-1}$) | $k_{nr}$ (x $10^6$ $s^{-1}$) | $k_r$ (x $10^4$ $s^{-1}$) | $k_{nr}$ (x $10^6$ $s^{-1}$) |
| Water | 6.7 | 8.4 | 7.3 | 8.0 | 4.9 | 7.0 |
| Methanol | 3.0 | 2.8 | 5.7 | 2.8 | 2.1 | 2.6 |
| Acetonitrile | 4.7 | 1.6 | 5.1 | 1.8 | 4.4 | 1.4 |
| Acetone | 3.4 | 1.5 | 6.3 | 1.8 | 4.7 | 1.3 |
| Dichloromethane | 4.2 | 1.4 | 3.2 | 1.1 | 8.3 | 0.8 |

Errors estimated to 10%.

Table 6. Parameters of deactivation of the excited $^3$MLCT state of Ru(II) complexes evaluated according to the Van Houten - Watts equation.

| Complex | Solvent | $E_a$ ($cm^{-1}$) | A ($s^{-1}$) | $k_i$ ($s^{-1}$) |
|---|---|---|---|---|
| $[Ru(phen)_2(TAPHAT)]^{2+}$ **1** | BuCN | 820 | $1.38\ 10^7$ | $9.91\ 10^5$ |
| $[Ru(phen)_2(TAPHAT)Ru(phen)_2]^{4+}$ **2** | BuCN | 1100 | $6.04\ 10^7$ | $1.37\ 10^6$ |
| $[Ru(bpy)_3]^{2+}$ [74] | $CH_3CN$ | 3800 | $5.8\ 10^{13}$ | $5.57\ 10^5$ |
| $[Ru(TAP)_2(phen)]^{2+}$ [91] | $CH_3CN$ | 3700 | $1.1\ 10^{13}$ | $3.31\ 10^5$ |
| $[Ru(TAP)_2(phen)]^{2+}$ [91] | BuCN | 417/3120 | $1.2\ 10^6/1.0\ 10^{13}$ | $2.0\ 10^5$ |
| $[Ru(TAP)_3]^{2+}$ [71] | $CH_3CN$ | 3150 | $7.3\ 10^{13}$ | $1.71\ 10^6$ |

Table 7. Quenching rate constants determined at pH5 under air in the presence of 150 mM sodium chloride and 10 mM phosphate buffer.

| | $\tau_0$ (ns) | $E_{red}$* (V vs SCE) | $H_2Q$ ($M^{-1}.s^{-1}$) | GMP ($M^{-1}.s^{-1}$) |
|---|---|---|---|---|
| $[Ru(phen)_2(TAPHAT)]^{2+}$ **1** | 113 | 1.17 | $2.53\ 10^9$ | $6.24\ 10^8$ |
| $[Ru(phen)_2(TAPHAT)Ru(phen)_2]^{4+}$ **2** | 122 | 1.19 | $2.17\ 10^9$ | $6.54\ 10^8$ |
| $[Ru(phen)_2(HAT)]^{2+}$ | 136 | 0.89 | $1.76\ 10^9$ | $0.24\ 10^8$ [a] |
| $[Ru(phen)_2(TAP)]^{2+}$ | 117 | 0.88 | $1.55\ 10^9$ | ---[b] |
| $[Ru(phen)_3]^{2+}$ | 526 | 0.71 | $7.46\ 10^7$ | ---[b] |

(a) Value from literature for the quenching at pH 7 in 0.1 M phosphate buffer. [92] (b) No quenching is occurring. $\tau_0$ is the luminescence lifetime under air.

## Conclusions

The new extended and highly electron-deficient ligand TAPHAT has been successfully synthesized by condensation between 1,4,5,8-tetraazaphenanthrene-9,10-dione (**TAPdione**) and 1,4,5,8-tetraazaphenanthrene-9,10-diamine (**diNH$_2$TAP**). The synthesis of **TAPdione**, a key intermediate for the development of highly π-accepting building blocks, proceeds through a ten-step procedure involving a final (bisacetoxy)iodobenzene oxidation. This allows for the synthesis of the desired TAPHAT ligand by a subsequent condensation with **diNH$_2$TAP**. An alternative synthetic path for the TAPHAT ligand is also developed by auto-condensation of **diNH$_2$TAP** in water by bubbling oxygen. This reaction is also used to perform chemistry on the complexes themselves, allowing for the isolation of two novel ruthenium(II) complexes, $[Ru(phen)_2(TAPHAT)]^{2+}$ **1** and $[Ru(phen)_2(TAPHAT)Ru(phen)_2]^{4+}$ **2**, in almost quantitative yields. These complexes are characterized using NMR spectroscopy and high-resolution mass spectrometry. This novel, green and easy synthetic procedure should modernize reactions in which the preparation of pyrazine cores is needed, not only for the synthesis of useful ligands but also for the formation of desired transition metal complexes.

The photophysical and electrochemical properties of these two complexes are investigated and compared with reference complexes. The most interesting and striking property evidenced for these complexes is that up to three reduction waves are centered on the ligand TAPHAT. This means that both the mono- and the binuclear complexes show the ability to store at least three electrons on the same TAPHAT ligand. The first reduction wave occurs at a potential of about -0.55V vs SCE, which is unusually high for complexes of this type. We also showed that the chelation of a second $\{Ru(phen)_2\}$ moiety to the bis-chelating site of TAPHAT plays a role in the excited-state stabilization, as evidenced by $(H/D)_2O$ isotopic effects. Finally, the combination of the data obtained in this work highlights the photo-oxidizing properties of $[Ru(phen)_2(TAPHAT)]^{2+}$ and $[Ru(phen)_2(TAPHAT)Ru(phen)_2]^{4+}$ as quenching experiments demonstrated that the excited states of these complexes are able to oxidize guanine, making them potential tools for biomedical application. Future work will investigate the possibility of intercalating mononuclear complex **1** within DNA, giving rise to a photoreactive luminophore with an excited-state localized on the intercalating ligand. Complexes **1** and **2** will also be used in proton-coupled electron transfer (PCET) applications as well as the investigation of accumulating the redox equivalents on the TAPHAT ligand in a photochemical way. The use of the trisdentate chelation site to build polynuclear architectures will also be investigated.

## Experimental section

### Instrumentation

The $^1$H NMR spectra for complexes **1** and **2** were recorded at room temperature with a Bruker Avance-300. (High Resolution) mass spectrometry analysis were performed on a Waters QToF-US mass spectrometer equipped with an Electrospray Ionization source (positive ion mode). The mass spectra were recorded using the time-of-flight analyzer with a FWHM resolution of 10.000 (*m/z* 500). The samples are solubilized in a water/methanol 1/1 solution (1 mg/mL) and

directly infused within the ESI capillary (5 µL/min). Typical source conditions were: capillary voltage, 3.1 kV; cone voltage, 30 V; source temperature, 80°C, desolvation temperature, 120 °C. Accurate mass measurements were obtained using sodium iodide clusters (NaI solution in water/isopropanol) as the lock mass ions. Infrared spectra were recorded with an alpha-Bruker in ATR mode on a germanium crystal.

Cyclic and square wave voltammetry were carried out on a platinum disk working electrode in dried acetonitrile with tetrabutylammonium perchlorate (0.1 mol $L^{-1}$) as supporting electrolyte. The potential of the working electrode was controlled by an Autolab PGSTAT 100 potentiostat through a PC interface with a scan rate of 100 mV $s^{-1}$ between -2 and +2 V versus SCE. The counter electrode was a platinum disk and the reference electrode a saturated calomel electrode (SCE). All the measurements were performed in a single compartment cell. The concentration of the complexes was 0.5-3 x $10^{-3}$ mol $L^{-1}$. Dilution experiments were performed by progressively adding electrolyte solution and purging for an additional 10 minutes prior to every measurement.

The UV-Vis absorption spectra were recorded on a Perkin-Elmer Lambda UV-Vis spectrophotometer and the emission spectra with a Shimadzu RF-5001 PC spectrometer (detection: Hamamatsu R-928 red-sensitive photomultiplier tube, excitation source: xenon lamp 250 W). The emission spectra were corrected for the instrument response. The determination of the molar absorption coefficients was performed by weight and absorption at several dilutions measurements.

Emission quantum yields were determined under argon by comparative actinometry using $[Ru(bpy)_3]^{2+}$ in water chosen as the standard luminophore [93] and was corrected for the solvent's refractive index.

The luminescence lifetimes were measured by the time-correlated single photon counting (TC-SPC) technique with the Edinburgh Instruments FL900 spectrometer equipped with a laser diode (λ = 439 nm, pulse = 100 ps). The samples were thermostated at 20 ± 2 °C with a Haake Model NB22 temperature controller. The data were collected by a multichannel analyzer (2048 channels) with a number of counts in the first channel (t = 0) at the minimum equal to $10^4$. The resulting decays were fitted to the exponential functions using the original manufacturer software package (Edinburgh Instruments). The reduced $\chi^2$, weighted residuals and autocorrelation function were employed to judge the quality of the fits.

Stern-Volmer measurements were performed under air in a quartz cell of 10 mm optical path length that was filled with 2 mL of solution buffered at the desired pH containing the desired complex with an absorbance of 0.1 at 440 nm (about 10 µM), 150 mM NaCl, 10 mM phosphate and the quencher with a concentration of 20 mM for GMP and 25 mM for $H_2Q$. The quencher concentration was gradually diluted without changing the concentration of the other compounds.

**Materials**

9-methoxy-1,4,5,8-tetraazaphenanthrene [48], 9,10-diamino-1,4,5,8-tetraazaphenanthrene [27] and $[Ru(phen)_2(diNH_2TAP)]^{2+}$ [42] were synthesized according to procedures reported previously. All other reagents were commercially available, with purity greater than 98% and were used as received. Electrochemical grade $TBAClO_4$ was used for the electrochemical measurements. Solvents used for photophysical measurements were of spectrophotometric grade.

**9-hydroxy-1,4,5,8-tetraazaphenanthrene.** 9-methoxy-1,4,5,8-tetraazaphenanthrene (200 mg, 0.94 mmol) was dissolved in 10 mL acetic acid. The solution was heated at 60°C and 2 mL of HI were added dropwise. The solution was heated at 60°C for two hours and then heated to reflux for an additional two hours. After reaction, the reaction mixture was brought to room temperature and poured into 30 mL of iced water. The latter was neutralized with 50% sodium hydroxide and the precipitate was collected by filtration and washed with water. The precipitate was redissolved in 50 mL THF/H2O 1:1 and concentrated under vacuum. This procedure was repeated several times until the collecting flask of the rotary evaporator becomes colorless. A light brown powder was finally obtained (160 mg, 85%).

$^1$H NMR (300.1 MHz, δ-MeOD): 7.58 (1H, s), 9.01 (2H, d, J = 2.4 Hz), 9.23 (2H, dd, J = 2.1 Hz).$^{13}$C NMR (75.5 MHz, δ-MeOD): 147.7; 147.3; 146.8; 146.3; 142.0; 141.0; 108.5. ESI-MS : *m/z* 199.1 (M + $H^+$, 100%), 221.2 (M + $Na^+$, 25%). IR (neat, $\nu_{max}$/$cm^{-1}$): 3240, 1607, 1515, 1455, 1338, 1317, 1242.

**1,4,5,8-tetraazaphenanthrene-9,10-dione.** 9-hydroxy-1,4,5,8-tetraazaphenanthrene (200 mg, 1,01 mmol) was dissolved in 20 mL of a 3:1 acetonitrile/water mixture. The mixture was stirred at room temperature and (bisacetoxy)iodobenzene (709 mg, 2,2 mmol) was added in one portion. After 24 h, the reaction mixture was filtered and concentrated under reduced pressure. The residue was washed with diethyl ether and filtered. The desired 1,4,5,8-tetraazaphenanthrene-9,10-dione was obtained as a light orange solid (177 mg, 83%).

$^1$H NMR (300.1 MHz, δ-DMSO-$d_6$): 8.73 (2H, d, J = 2.7 Hz), 8.78 (2H, d, J = 2.7 Hz). $^{13}$C NMR (75.5 MHz, δ-DMSO-$d_6$): 180.2 ; 165.9 ; 145.6 ; 145.2 ; 143.8. ESI-MS: *m/z* 213.1 (20%, M + $H^+$), 235.0 (100%, M + $Na^+$), 447.1 (35%, 2M + $Na^+$). IR (neat, $\nu_{max}$/$cm^{-1}$): 1688 ; 1524, 1356 ; 1315 ; 848.

**1,4,5,8-tetraazaphenanthrene[9,10-b]1,4,5,8,9,12-hexaazatriphenylene (TAPHAT).2$H_2O$**

**Route A.** 9,10-diamino-1,4,5,8-tetraazaphenanthrene (60mg, 0,285 mmol) and 1,4,5,8-tetraazaphenanthrene-9,10-dione (60 mg, 0,286 mmol) were refluxed in 8 mL of EtOH/AcOH/H2O 10 :4 :1. The medium color changed from reddish to pale yellow. Appearance of a precipitate was also quickly noticed. The reaction was followed by TLC ($Al_2O_3$, $CHCl_3$ :EtOH 98 :2). After 4 h, the reaction was stopped and the medium was cooled to room temperature. 10 mL of water were added at this point and the precipitate was collected by centrifugation. The precipitate was washed twice with water, ethanol and diethyl ether. TAPHAT was

obtained as a grey solid and was used without further purification (87 mg, 79%).

**Route B.** 9,10-diamino-1,4,5,8-tetraazaphenanthrene (200 mg, 0.94 mmol) and sodium acetate (770 mg, 9.4 mmol) were stirred in 15 mL of distilled water. The reaction medium was heated to reflux and a stream of oxygen was bubbled in the reaction mixture using a needle. The reaction was maintained for 6 h. The color of the medium changed from reddish to pale yellow. After 6 h, the reaction was cooled to room temperature and the solid was collected by centrifugation. The solid was washed twice with water, ethanol and diethyl ether. TAPHAT was obtained as a grey solid (370 mg, 92%).

EI-MS: *m/z* 389.1 ($M + H^+$, 100%), 411.0 ($M + Na^+$, 40%), 427.0 ($M + K^+$, 25%). Anal. Calcd for $C_{20}H_{12}N_{10}O_2$: C, 56.60; H, 2.85; N, 33.01. Found: C, 55.98; H, 2.96; N, 33.03 %

**$[Ru(phen)_2(TAPHAT)]^{2+}.2Cl^-$**. $Ru(phen)_2(diNH_2TAP)]^{2+}.2Cl^-$ (100 mg, 0,134 mmol) and 1,4,5,8-tetraazaphenanthrene-9,10-dione (37,0 mg, 0,174 mmol) were refluxed in 15 mL $EtOH/H_2O$ 7:3 under argon atmosphere. The reaction was monitored by TLC ($Al_2O_3$, $CH_3CN/H_2O$ 9 :1). After reaction, the mixture was cooled to room temperature and the solvent was evaporated. The residue was purified by column chromatography on alumina ($CH_3CN/H_2O$ 90/10 to 80/20). The product was obtained with a yield of 42%.

**$[Ru(phen)_2(TAPHAT)]^{2+}.2PF_6^-$**. $[Ru(phen)_2(diNH_2TAP)]^{2+}.2Cl^-$ (100 mg, 0,134 mmol), 9,10-di$NH_2$-1,4,5,8-tetraazaphenanthrene (57 mg, 0,269 mmol) and sodium acetate (66 mg, 0,804 mmol) were stirred in 4 mL of distilled water. The reaction mixture was refluxed and oxygen was bubbled through the solution using a needle. The reflux was maintained for 6 h. After reaction, the mixture was cooled to room temperature and centrifuged. The precipitate (TAPHAT) was washed twice with water. The aqueous layers were collected and concentrated to a volume of about 2 mL. A saturated solution of $NH_4PF_6$ was then added to precipitate the complex. The mixture was centrifuged and the precipitate was washed twice with water, ethanol and diethyl ether, yielding the desired complex (142 mg, 93%).

$^1H$ NMR (300.1 MHz, $\delta$ -$CD_3CN$) : 7.70 (4H, dd, $H_{3,8}$, J = 1.8, 3.9 Hz), 8.03 (2H, dd, $H_{9/2}$, J = 0.9, 3.9 Hz), 8.29 (2H, dd, $H_{2/9}$), 8.30 (4H, s, $H_{5,6}$), 8.34 (2H, d, H$\alpha$, J = 2.7 Hz), 8.68 (2H, m, $H_{4/7}$), 8.70 (2H, m, $H_{7/4}$), 9.09 (2H, d, Hß, J = 2.4 Hz), 9.35 (2H, d, H$\gamma$, J = 1.2 Hz), 9.37 (2H, d, H$\varepsilon$, J = 1.2 Hz). ESI-MS: *m/z* 995.08 (100%, $[M^{2+} + PF_6^-]^+$), 850.12 (25%, $[M^{2+} - H^+]^+$). HRMS (ESI): $[M^+]$ calculated for $C_{44}H_{24}N_{14}F_6P^{96}Ru$ *m/z* 989.1026; found *m/z* 989.1028.

**$[Ru(phen)_2(TAPHAT)Ru(phen)_2]^{4+}.4PF_6^-$.**

$[Ru(phen)_2(diNH_2TAP)]^{2+}.2Cl^-$ (100 mg, 0,134 mmol) and sodium acetate (66 mg, 0,804 mmol) were stirred in 4 mL of distilled water. The reaction mixture was refluxed and oxygen was bubbled through the solution using a needle. The reaction was kept refluxing for 8 h. After reaction, the mixture was cooled to room temperature and centrifuged. The supernatant was concentrated to a volume of about 2 mL and a saturated solution of $NH_4PF_6$ was then added to precipitate the complex. The mixture was centrifuged and the precipitate was washed twice with water, ethanol and diethyl ether, yielding the desired complex (242 mg, 95%).

$^1H$ NMR (300.1 MHz, δ-$CD_3CN$): 7.71 (8H, dd, $H_{3,8}$, J = 3.9 Hz), 8,02 (4H, d, $H_{9/2}$, J = 5.2 Hz), 8.30 (12H, 2s, $H_{2/9}$ and $H_{5,6}$), 8.39 (4H, $S_{br}$, H$\alpha$), 8.68 (4H, dd, $H_{4/7}$), 8.70 (4H, dd, $H_{7/4}$), 9.12 (4H, $S_{br}$, Hβ). HRMS (ESI): $[M^{3+}]$ calculated for $C_{68}H_{40}N_{18}F_6P^{96}Ru_2^{3+}$ *m/z* 483.0488; Found *m/z* 483.0437.

## Acknowledgements

L.T.-G. thanks the “Fonds pour la Formation à la Recherche dans l'Industrie et dans l'Agriculture” (FRIA) for funding. P.G. and J.D.W thank the « Fonds National pour la Recherche Scientifique » for financial support for the acquisition of the Waters QToF Premier and Waters Synapt G3-Si mass spectrometer. C.M. thanks the « Fonds National pour la Recherche Scientifique » for continuous support. This research was supported by the “Fonds National pour la Recherche Scientifique” contracts 2.4530.12 and 2.4615.11 and the COST action CM 1202.

## Notes and references

‡ Structures of the different ligands discussed in this paper are depicted in Figure S1 in supplementary information.

§ Determined at 0.213 bar of $O_2$, Handbook of Photochemistry, 3rd Ed, 2006, p. 544.

1 A. Hagfeldt, G. Boschloo, L. Sun, L. Kloo and H. Pettersson, *Chem. Rev.*, 2010, **110,** 6595-6663.

2 J. J. Concepcion, J. W. Jurss, M. K. Brennaman, P. G. Hoertz, A. OT. Patrocinio, M. aYN. Iha, J. L. Templeton and T. J. Meyer, *Acc. Chem. Res.*, 2009, **42,** 1954-1965.

3 M. D. Kärkäs, E. V. Johnston, E. A. Karlsson, BL. Lee, T. Åkermark, M. Shariatgorji, L. Ilag, Ö. Hansson, JE. Bäckvall and B. Åkermark, *Chem. Eur. J.*, 2011, **17,** 7953-7959.

4 F. Puntoriero, A. Sartorel, M. Orlandi, G. L. Ganga, S. Serroni, M. Bonchio, F. Scandola and S. Campagna, *Coord. Chem. Rev.*, 2011, **255,** 2594-2601.

5 D. M. Schultz and T. P. Yoon, *Science*, 2014, **343,** 1239176-1239176.

6 T. P. Yoon, M. A. Ischay and J. Du, *Nat. Chem.*, 2010, **2,** 527-532.

7 B. D. Sherman, M. V. Sheridan, KR. Wee, S. L. Marquard, D. Wang, L. Alibabaei, D. L. Ashford and T. J. Meyer, *J. Am. Chem. Soc.*, 2016, **138,** 16745-16753.

8 J. MR. Narayanam and C. RJ. Stephenson, *Chem. Soc. Rev.*, 2011, **40,** 102-113.

9 J. Xuan and WJ. Xiao, *Angew. Chem., Int. Ed.*, 2012, **51,** 6828-6838.

10 C. K. Prier, D. A. Rankic and D. WC. MacMillan, *Chem. Rev.*, 2013, **113,** 5322-5363.

11 D. Ravelli, S. Protti and M. Fagnoni, *Chem. Rev.*, 2016, **116,** 9850-9913.

12 M. Kuss-Petermann, M. Orazietti, M. Neuburger, P. Hamm and O. S. Wenger, *J. Am. Chem. Soc.*, 2017.

13 L. Hammarstrom, *Acc. Chem. Res.*, 2015, **48,** 840-850.

 

14 M. Orazietti, M. Kuss-Petermann, P. Hamm and O. S. Wenger, *Angew. Chem., Int. Ed.*, 2016, **55,** 9407-9410.

15 R. Konduri, N. R. de Tacconi, K. Rajeshwar and F. M. MacDonnell, *J. Am. Chem. Soc.*, 2004, **126,** 11621-11629.

16 R. Konduri, H. Ye, F. M. MacDonnell, S. Serroni, S. Campagna and K. Rajeshwar, *Angew. Chem., Int. Ed.*, 2002, **41,** 3185-3187.

17 M. R. Gill and J. A. Thomas, *Chem. Soc. Rev.*, 2012, **41,** 3179-3192.

18 A. C. Komor and J. K. Barton, *Chem. Commun.*, 2013, **49,** 3617-3630.

19 L. Marcélis, J. Ghesquière, K. Garnir, A. Kirsch-De Mesmaeker and C. Moucheron, *Coord. Chem. Rev.*, 2012, **256,** 1569-1582.

20 C. J. Cardin, J. M. Kelly and S. J. Quinn, *Chem. Sci.*, 2017.

21 J. P. Hall, F. E. Poynton, P. M. Keane, S. P. Gurung, J. A. Brazier, D. J. Cardin, G. Winter, T. Gunnlaugsson, I. V. Sazanovich, M. Towrie, C. J. Cardin, J. M. Kelly and S. J. Quinn, *Nat. Chem.*, 2015, **7,** 961-967.

22 P. M. Keane, F. E. Poynton, J. P. Hall, I. V. Sazanovich, M. Towrie, T. Gunnlaugsson, S. J. Quinn, C. J. Cardin and J. M. Kelly, *Angew. Chem., Int. Ed.*, 2015, **54,** n/a--n/a.

23 J. P. Hall, D. Cook, S. R. Morte, P. McIntyre, K. Buchner, H. Beer, D. J. Cardin, J. A. Brazier, G. Winter, J. M. Kelly and C. J. Cardin, *J. Am. Chem. Soc.*, 2013, **135,** 12652-12659.

24 L. Troian-Gautier and C. Moucheron, *Molecules*, 2014, **19,** 5028-5087.

25 A. E. Friedman, J. C. Chambron, J. P. Sauvage, N. J. Turro and J. K. Barton, *J. Am. Chem. Soc.*, 1990, **112,** 4960-4962.

26 B. T. Patterson, J. Grant Collins, F. M. Foley and F. Richard Keene, *J. Chem. Soc., Dalton Trans.*, 2002, 4343-4350.

27 C. Moucheron, A. Kirsch-De Mesmaeker and S. Choua, *Inorg. Chem.*, 1997, **36,** 584-592.

28 S. Rickling, L. Ghizdavu, F. Pierard, P. Gerbaux, M. Surin, P. Murat, E. Defrancq, C. Moucheron and A. Kirsch-De Mesmaeker, *Chem. Eur. J.*, 2010, **16,** 3951-3961.

29 S. Campagna, F. Puntoriero, F. Nastasi, G. Bergamini and V. Balzani. Photochemistry and Photophysics of Coordination Compounds: Ruthenium. In *Photochemistry and Photophysics of Coordination Compounds I;* V. Balzani, S. Campagna, Eds.;, 2007; Vol. 280, pp 117-214.

30 G. F. Manbeck and K. J. Brewer, *Coord. Chem. Rev.*, 2013, **257,** 1660-1675.

31 R. W. Harrigan, G. D. Hager and G. A. Crosby, *Chem. Phys. Lett.*, 1973, **21,** 487-490.

32 J. N. Demas and D. G. Taylor, *Inorg. Chem.*, 1979, **18,** 3177-3179.

33 B. Durham, J. V. Caspar, J. K. Nagle and T. J. Meyer, *J. Am. Chem. Soc.*, 1982, **104,** 4803-4810.

34 P. Dongare, B. DB. Myron, L. Wang, D. W. Thompson and T. J. Meyer, *Coord. Chem. Rev.*, 2017, **345,** 86-107.

35 N. H. Damrauer, G. Cerullo, A. Yeh, T. R. Boussie, C. V. Shank and J. K. McCusker, *Science*, 1997, **275,** 54-57.

36 C. Turro, S. H. Bossmann, Y. Jenkins, J. K. Barton and N. J. Turro, *J. Am. Chem. Soc.*, 1995, **117,** 9026-9032.

37 R. B. Nair, B. M. Cullum and C. J. Murphy, *Inorg. Chem.*, 1997, **36,** 962-965.

38 E. JC. Olson, D. Hu, A. Hörmann, A. M. Jonkman, M. R. Arkin, E. DA. Stemp, J. K. Barton and P. F. Barbara, *J. Am. Chem. Soc.*, 1997, **119,** 11458-11467.

39 M. K. Brennaman, J. H. Alstrum-Acevedo, C. N. Fleming, P. Jang, T. J. Meyer and J. M. Papanikolas, *J. Am. Chem. Soc.*, 2002, **124,** 15094-15098.

40 M. K. Brennaman, T. J. Meyer and J. M. Papanikolas, *J. Phys. Chem. A*, 2004, **108,** 9938-9944.

41 J. Olofsson, B. Önfelt and P. Lincoln, *J. Phys. Chem. A*, 2004, **108,** 4391-4398.

42 A. Boisdenghien, C. Moucheron and A. Kirsch-De Mesmaeker, *Inorg. Chem.*, 2005, **44,** 7678-7685.

43 G. Pourtois, D. Beljonne, C. Moucheron, S. Schumm, A. Kirsch-De Mesmaeker, R. Lazzaroni and JL. Brédas, *J. Am. Chem. Soc.*, 2004, **126,** 683-692.

44 R. Nasielski-Hinkens, M. Benedek-Vamos, D. Maetens and J. Nasielski, *J. Organomet. Chem.*, 1981, **217,** 179-182.

45 B. Kohne and K. Praefcke, *Liebigs Ann. Chem.*, 1985, **1985,** 522-528.

46 D. Z. Rogers, *J. Org. Chem.*, 1986, **51,** 3904-3905.

47 M. Yamada, Y. Tanaka, Y. Yoshimoto, S. Kuroda and I. Shimao, *Bull. Chem. Soc. Jpn.*, 1992, **65,** 1006-1011.

48 R. Nasielski-Hinkens, M. Benedek-Vamos and D. Maetens, *J. Heterocycl. Chem.*, 1980, **17,** 873-876.

49 R. Saladino, V. Neri, E. Mincione and P. Filippone, *Tetrahedron*, 2002, **58,** 8493-8500.

50 V. Nair and A. Deepthi, *Chem. Rev.*, 2007, **107,** 1862-1891.

51 P. Kraft and W. Eichenberger, *Eur. J. Org. Chem.*, 2003, **2003,** 3735-3743.

52 JT. Zhang, W. Dai and R. G. Harvey, *J. Org. Chem.*, 1998, **63,** 8125-8132.

53 B. Ghebremariam and S. Matile, *Tetrahedron Lett.*, 1998, **39,** 5335-5338.

54 M. Node, K. Nishide, K. Fuji and E. Fujita, *J. Org. Chem.*, 1980, **45,** 4275-4277.

55 L. Testaferri, M. Tiecco, M. Tingoli, D. Chianelli and M. Montanucci, *Tetrahedron*, 1982, **38,** 3687-3692.

56 L. Troian-Gautier, J. De Winter, P. Gerbaux and C. Moucheron, *J. Org. Chem.*, 2013, **78,** 11096-11101.

57 H. M. Gajiwala and R. Zand, *Polymer*, 2000, **41,** 2009-2015.

58 V. Balzani, F. Bolletta, M. T. Gandolfi and M. Maestri. Bimolecular electron transfer reactions of the excited states of transition metal complexes. In *Topics in Current Chemistry;* Springer-Verlag; pp 1-64.

59 L. Jacquet and A. Kirsch-De Mesmaeker, *J. Chem. Soc., Faraday Trans.*, 1992, **88,** 2471-2480.

60 S. Campagna, S. Serroni, S. Bodige and F. M. MacDonnell, *Inorg. Chem.*, 1999, **38,** 692-701.

61 B. Elias, L. Herman, C. Moucheron and A. Kirsch-De Mesmaeker, *Inorg. Chem.*, 2007, **46,** 4979-4988.

62 G. Piraux, L. Bar, M. Abraham, T. Lavergne, H. Jamet, J. Dejeu, L. Marcélis, É. Defrancq and B. Elias, *Chem. Eur. J.*, 2017.

63 J. M. Aslan, D. J. Boston and F. M. MacDonnell, *Chem. Eur. J.*, 2015, **21,** 17314-17323.

64 R. O. Lezna, N. RD. Tacconi and F. MacDonnell, *ECS Transactions*, 2008.

65 J. M. Aslan, M. Yousufuddin, D. J. Boston and F. M. MacDonnell, *Inorg. Chim. Acta*, 2017, **454,** 216-221.

66 MJ. Kim, R. Konduri, H. Ye, F. M. MacDonnell, F. Puntoriero, S. Serroni, S. Campagna, T. Holder, G. Kinsel and K. Rajeshwar, *Inorg. Chem.*, 2002, **41,** 2471-2476.

67 K. L. Wouters, N. R. de Tacconi, R. Konduri, R. O. Lezna and F. M. MacDonnell, *Photosynth. Res.*, 2006, **87,** 41-55.

68 J. Bolger, A. Gourdon, E. Ishow and JP. Launay, *J. Chem. Soc., Chem. Commun.*, 1995, 1799-1800.

69 J. Bolger, A. Gourdon, E. Ishow and JP. Launay, *Inorg. Chem.*, 1996, **35,** 2937-2944.

70 D. Garcìa-Fresnadillo, Y. Georgiadou, G. Orellana, A. M. Braun and E. Oliveros, *Helv. Chim. Acta*, 1996, **79,** 1222-1238.

71 A. Masschelein, L. Jacquet, A. Kirsch-De Mesmaeker and J. Nasielski, *Inorg. Chem.*, 1990, **29,** 855-860.

72 J. Van Houten and R. J. Watts, *J. Am. Chem. Soc.*, 1976, **98,** 4853-4858.

73 R. Battino, T. R. Rettich and T. Tominaga, *J. Phys. Chem. ref. Data*, 1983, **12,** 163-178.

74 J. V. Caspar and T. J. Meyer, *J. Am. Chem. Soc.*, 1983, **105,** 5583-5590.

75 G. H. Allen, R. P. White, D. P. Rillema and T. J. Meyer, *J. Am. Chem. Soc.*, 1984, **106,** 2613-2620.

76 F. Barigelletti, A. Juris, V. Balzani, P. Belser and A. Von Zelewsky, *Inorg. Chem.*, 1983, **22,** 3335-3339.

77 J. D. Knoll, B. A. Albani and C. Turro, *Acc. Chem. Res.*, 2015, **48,** 2280-2287.

78 Y. Sun, Y. Liu and C. Turro, *J. Am. Chem. Soc.*, 2010, **132,** 5594-5595.

79 M. Rebarz, L. Marcélis, M. Menand, D. Cornut, C. Moucheron, I. Jabin and A. Kirsch-De Mesmaeker, *Inorg. Chem.*, 2014, **53,** 2635-2644.

80 W. F. Wacholtz, R. A. Auerbach and R. H. Schmehl, *Inorg. Chem.*, 1986, **25,** 227-234.

81 R. M. OĎonnell, P. G. Johansson, M. Abrahamsson and G. J. Meyer, *Inorg. Chem.*, 2013, **52,** 6839-6848.

82 P. Chen and T. J. Meyer, *Chem. Rev.*, 1998, **98,** 1439-1478.

83 L. A. Worl, R. Duesing, P. Chen, L. D. Ciana and T. J. Meyer, *J. Chem. Soc., Dalton Trans.*, 1991, 849.

84 K. Huang and A. Rhys, *Proceedings of the Royal Society of London A: Mathematical, Physical and Engineering Sciences*, 1950, **204,** 406-423.

85 R. F. Dallinger and W. H. Woodruff, *J. Am. Chem. Soc.*, 1979, **101,** 4391-4393.

86 P. G. Bradley, N. Kress, B. A. Hornberger, R. F. Dallinger and W. H. Woodruff, *J. Am. Chem. Soc.*, 1981, **103,** 7441-7446.

87 J. V. Caspar, T. D. Westmoreland, G. H. Allen, P. G. Bradley, T. J. Meyer and W. H. Woodruff, *J. Am. Chem. Soc.*, 1984, **106,** 3492-3500.

88 B. R. Eggins, *J. Chem. Soc. D*, 1969, **0,** 1267-1268.

89 S. Steenken and S. V. Jovanovic, *J. Am. Chem. Soc.*, 1997, **119,** 617-618.

90 L. Troian-Gautier, E. Mugeniwabagara, L. Fusaro, C. Moucheron, A. KD. Mesmaeker and M. Luhmer, *Inorg. Chem.*, 2016.

91 M. Rebarz, J. Ghesquière, A. Boisdenghien, E. Defrancq, C. Moucheron and A. Kirsch-De Mesmaeker, *Inorg. Chem.*, 2010, **49,** 10867-10874.

92 C. Moucheron, A. Kirsch-De Mesmaeker and J. M. Kelly, *J. Photochem. Photobiol. B Biol.*, 1997, **40,** 91-106.

93 A. Juris, V. Balzani, F. Barigelletti, S. Campagna, P. Belser and A. von Zelewsky, *Coord. Chem. Rev.*, 1988, **84,** 85-277.